

Pre-submission seminar

A study on the energy transfer of a body under fluid-elastic galloping

Supervisors:

Dr. Tan Boon Thong

Dr. Justin Leontini

Dr Huang Yew Mun



MONASH University
Malaysia

Flow induced vibrations can lead to structural failure



Source :[http://en.wikipedia.org/wiki/Tacoma_Narrows_Bridge_\(1940\)#mediaviewer/File:Image-Tacoma_Narrows_Bridge1.gif](http://en.wikipedia.org/wiki/Tacoma_Narrows_Bridge_(1940)#mediaviewer/File:Image-Tacoma_Narrows_Bridge1.gif)

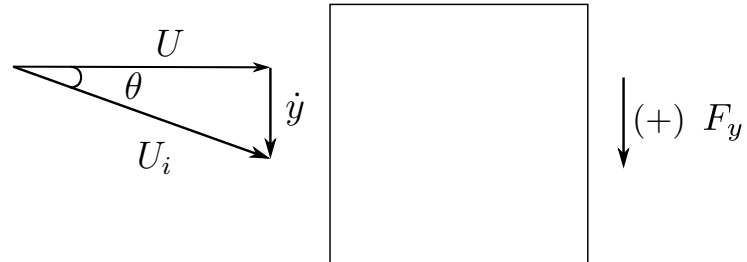


Source: <http://www.inmr.com/wp-content/uploads/2013/11/cover.jpg>

This project consist of 3 phases

- Phase 1: Understand the underpinning parameters and formulate the appropriate variables of the system.
- Phase 2: Study the frequency response of the system, and the relationship with the formulated variables.
- Phase 3: Optimisation of the energy transfer by controlling the fluid mechanics of the system.

Mechanism of galloping and Quasi-steady state hypothesis



U Freestream velocity

U_i Induced velocity

U_i Induced velocity

θ Induced angle

\dot{y} Transverse velocity

C_L Coefficient of lift

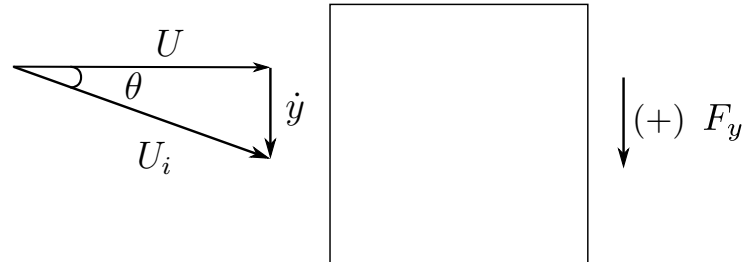
C_d Coefficient of drag

C_y Coefficient of transverse force

F_y Transverse force



Mechanism of galloping and Quasi-steady state hypothesis



U Freestream velocity

U_i Induced velocity

U_i Induced velocity

θ Induced angle

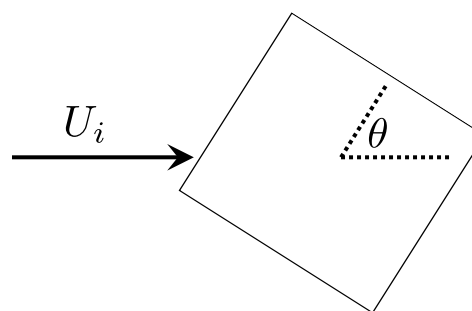
\dot{y} Transverse velocity

C_L Coefficient of lift

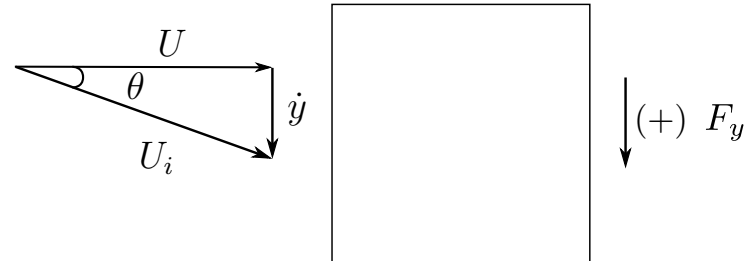
C_d Coefficient of drag

C_y Coefficient of transverse force

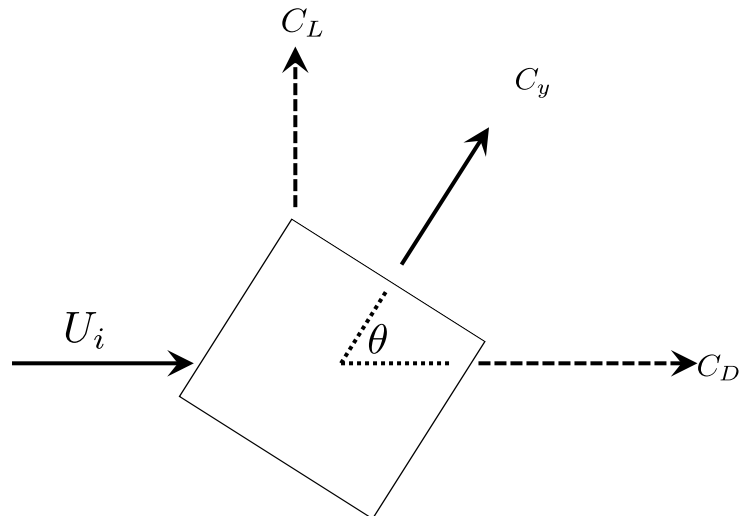
F_y Transverse force



Mechanism of galloping and Quasi-steady state hypothesis



U	Freestream velocity
U_i	Induced velocity
U_i	Induced velocity
θ	Induced angle
\dot{y}	Transverse velocity
C_L	Coefficient of lift
C_d	Coefficient of drag
C_y	Coefficient of transverse force
F_y	Transverse force



QSS model and mean power equations

$$m\ddot{y} + c\dot{y} + ky = \frac{1}{2}\rho U^2 \mathcal{A} \left(a_1 \left(\frac{\dot{y}}{U} \right) + a_3 \left(\frac{\dot{y}}{U} \right)^3 + a_5 \left(\frac{\dot{y}}{U} \right)^5 + a_7 \left(\frac{\dot{y}}{U} \right)^7 \right)$$

$$P_m = \frac{1}{T} \int_0^T (c\dot{y})\dot{y} dt$$

$$P_m = \frac{1}{T} \int_0^T F_y \dot{y} dt$$

QSS model and mean power equations

$$m\ddot{y} + c\dot{y} + ky = \frac{1}{2}\rho U^2 A \left(a_1 \left(\frac{\dot{y}}{U} \right) + a_3 \left(\frac{\dot{y}}{U} \right)^3 + a_5 \left(\frac{\dot{y}}{U} \right)^5 + a_7 \left(\frac{\dot{y}}{U} \right)^7 \right)$$

a_1, a_3, a_5, a_7	Coefficients of the polynomial to determine C_y
$A = DL$	Frontal area of the body
c	Damping constant
k	Spring constant
m	Mass of the body
U	Freestream velocity
ρ	Fluid density
y, \dot{y}, \ddot{y}	Transverse displacement, velocity and acceleration of the body

QSS model and mean power equations

$$m\ddot{y} + c\dot{y} + ky = \frac{1}{2}\rho U^2 \mathcal{A} \left(a_1 \left(\frac{\dot{y}}{U} \right) + a_3 \left(\frac{\dot{y}}{U} \right)^3 + a_5 \left(\frac{\dot{y}}{U} \right)^5 + a_7 \left(\frac{\dot{y}}{U} \right)^7 \right)$$

$$P_m = \frac{1}{T} \int_0^T (c\dot{y})\dot{y} dt$$

$$P_m = \frac{1}{T} \int_0^T F_y \dot{y} dt$$

P_m Mean power

F_y Instantaneous force normal to the flow

t time

Linearised QSS equation, natural time scales and non-dimensionalised parameters

$$m\ddot{y} + c\dot{y} + ky = \frac{1}{2}\rho U^2 \mathcal{A}a_1 \left(\frac{\dot{y}}{U} \right)$$

$$\lambda_{1,2} = -\frac{1}{2} \frac{c - \frac{1}{2}\rho U \mathcal{A}a_1}{m} \pm \frac{1}{2} \sqrt{\left[\frac{c - \frac{1}{2}\rho U \mathcal{A}a_1}{(m)} \right]^2 - 4\frac{k}{m}}.$$

$$\Pi_1 = 4\pi^2 m^{*2}/U^{*2}$$

$$\Pi_2 = c^* m^*$$

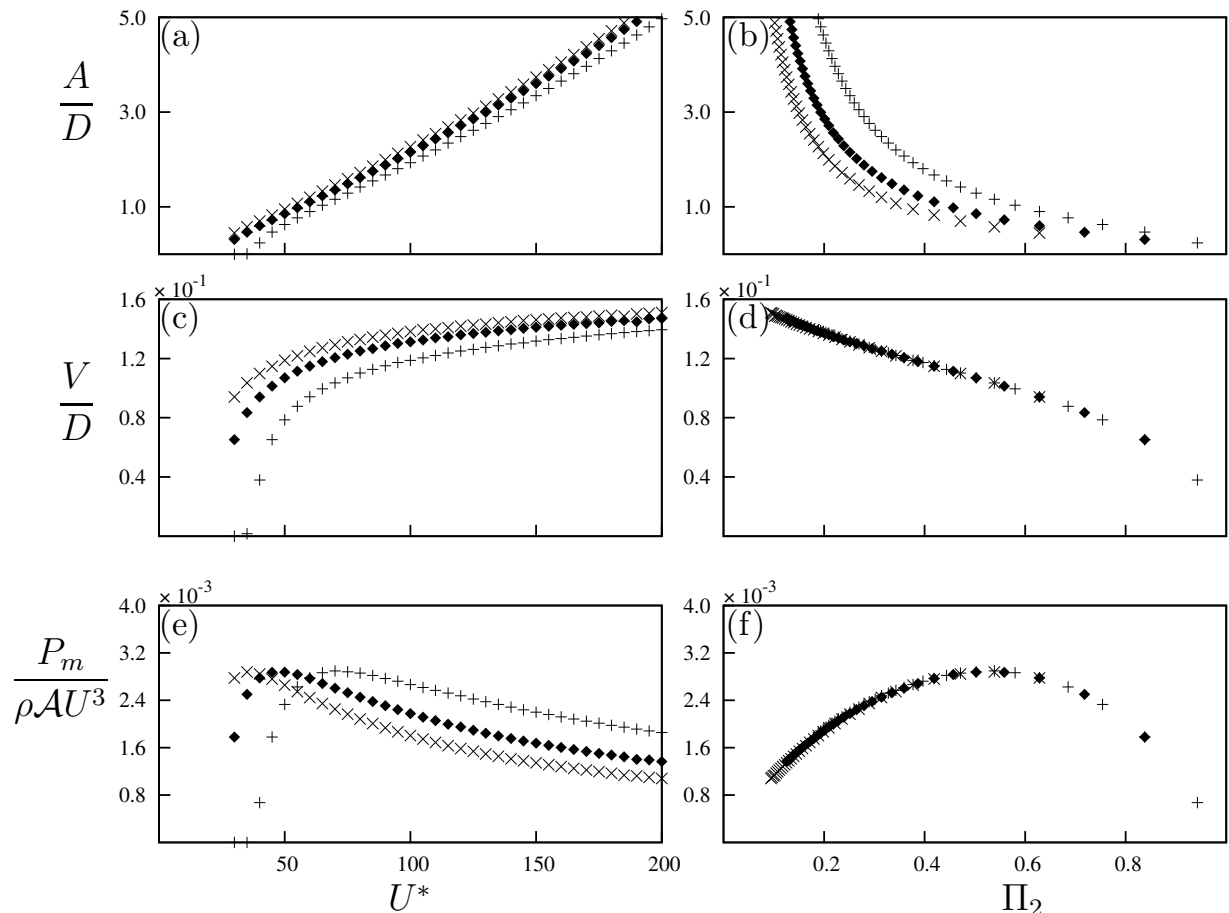
$$\begin{aligned} \lambda_{1,2} & \\ m^* &= m/\rho D^2 L \\ U^* &= U/fD \\ c^* &= cD/mU \\ \Pi_1 &= 4\pi^2 m^{*2}/U^{*2} \\ \Pi_2 &= c^* m^* \end{aligned}$$

Eigenvalues of linearised equation of motion
 Mass ratio
 Reduced velocity
 Non-dimensionalised damping factor
 Combined mass-stiffness parameter
 Combined mass-damping parameter

Classical VIV parameters vs. New Parameters

$$Re = 200 \\ m^* = 20$$

- $\zeta = 0.075$ (\times)
- $\zeta = 0.1$ (\blacklozenge)
- $\zeta = 0.15$ ($+$)



A Displacement amplitude
 V Velocity amplitude

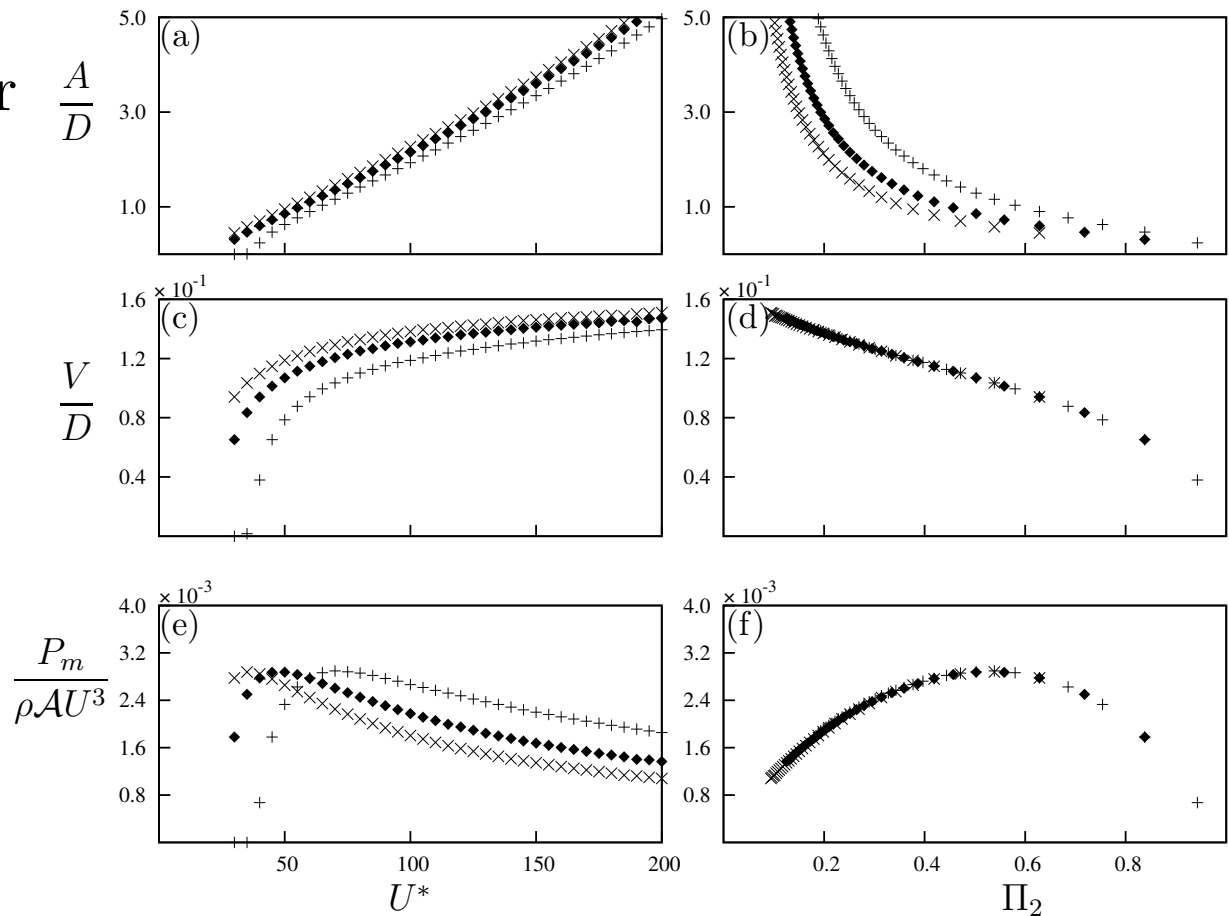
Classical VIV parameters vs. New Parameters

Π_2 provides a better collapse of the data

$$Re = 200$$

$$m^* = 20$$

- $\zeta = 0.075$ (\times)
- $\zeta = 0.1$ (\blacklozenge)
- $\zeta = 0.15$ ($+$)



A Displacement amplitude
 V Velocity amplitude

A good agreement between QSS and DNS results could be obtained at high Π_1

$Re = 200$

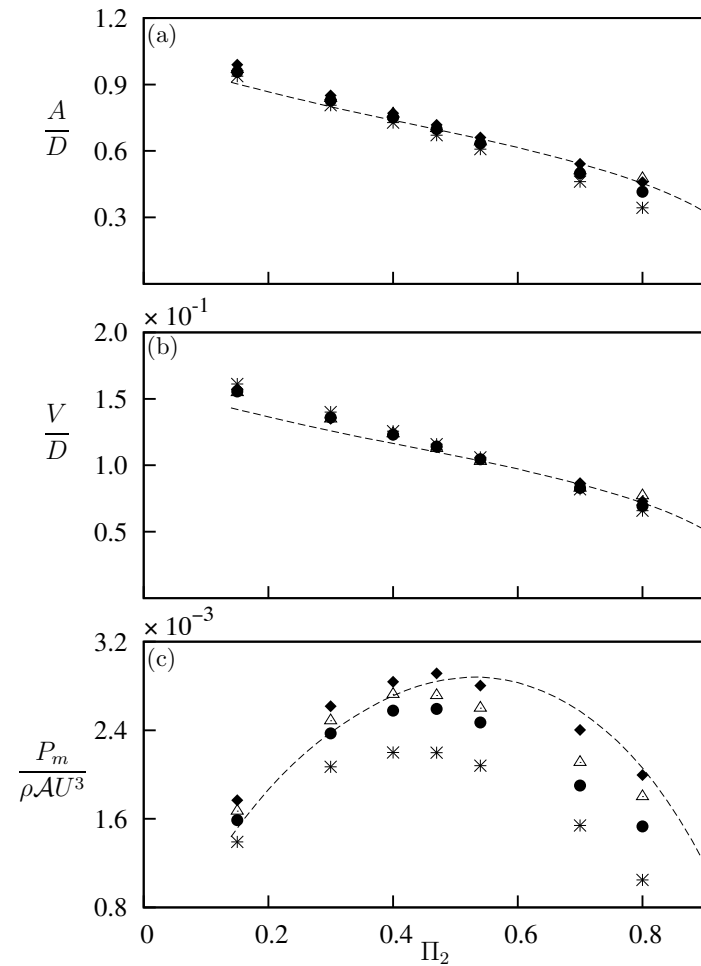
$\Pi_1 = 10$ ($m^* = 20.13$) (*)

$\Pi_1 = 60$ ($m^* = 49.31$) (●)

$\Pi_1 = 250$ ($m^* = 100.7$) (△)

$\Pi_1 = 1000$ ($m^* = 201.3$) (◆)

QSS data at $\Pi_1 = 10$ (---)



Clear wavelength is visible in the flow as Π_1 is increased

Vorticity plots at arbitrary instants at $\Pi_2 = 0.47$.

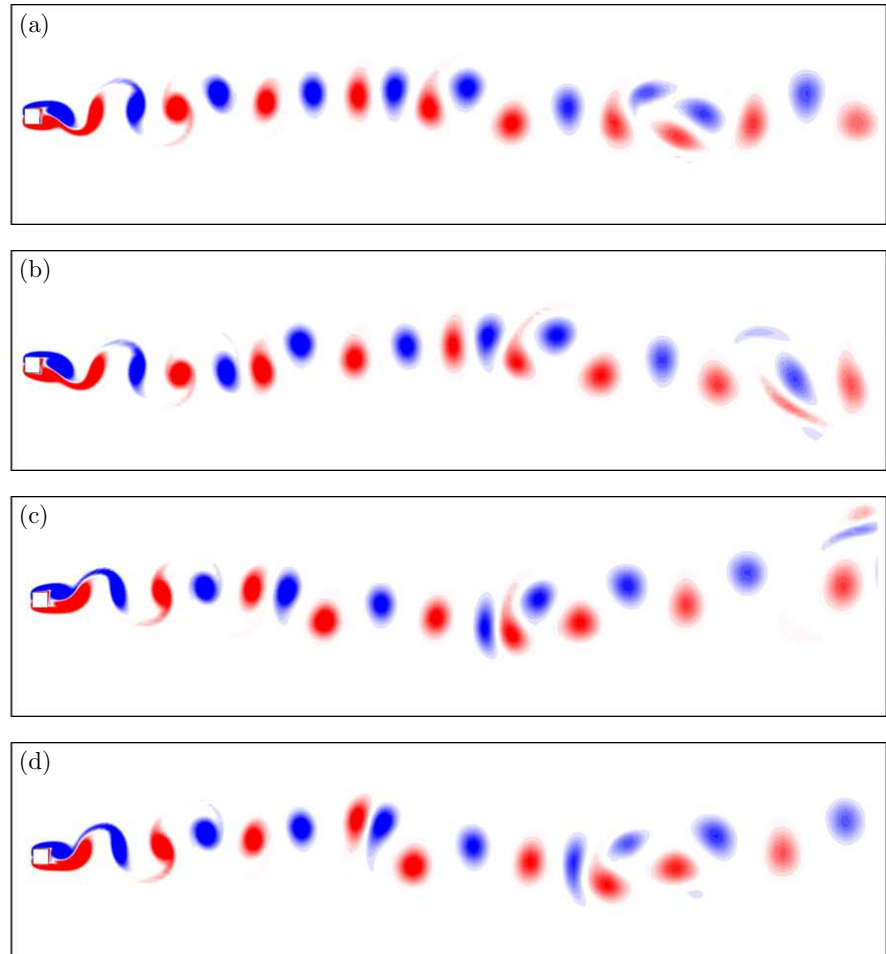
(a) $\Pi_1 = 10$

(b) $\Pi_1 = 60$

(a) $\Pi_1 = 250$

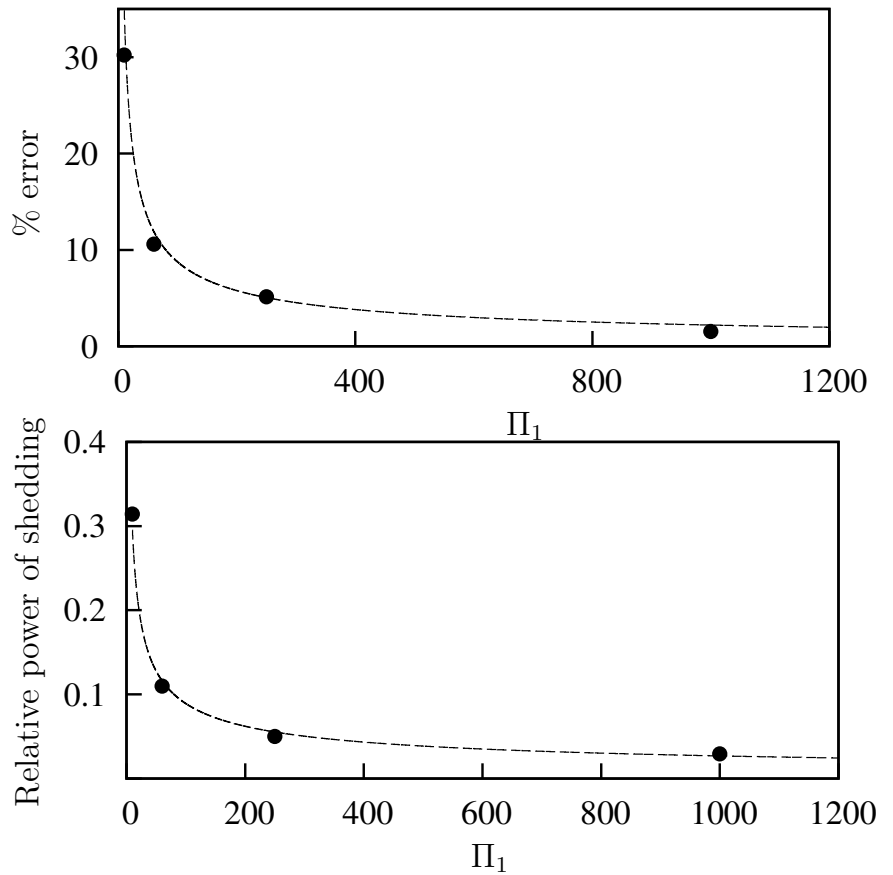
(d) $\Pi_1 = 1000$

$f_{input} = 0.025$



Relative power of shedding and % error of power between QSS and DNS is an inverse function of Π_1

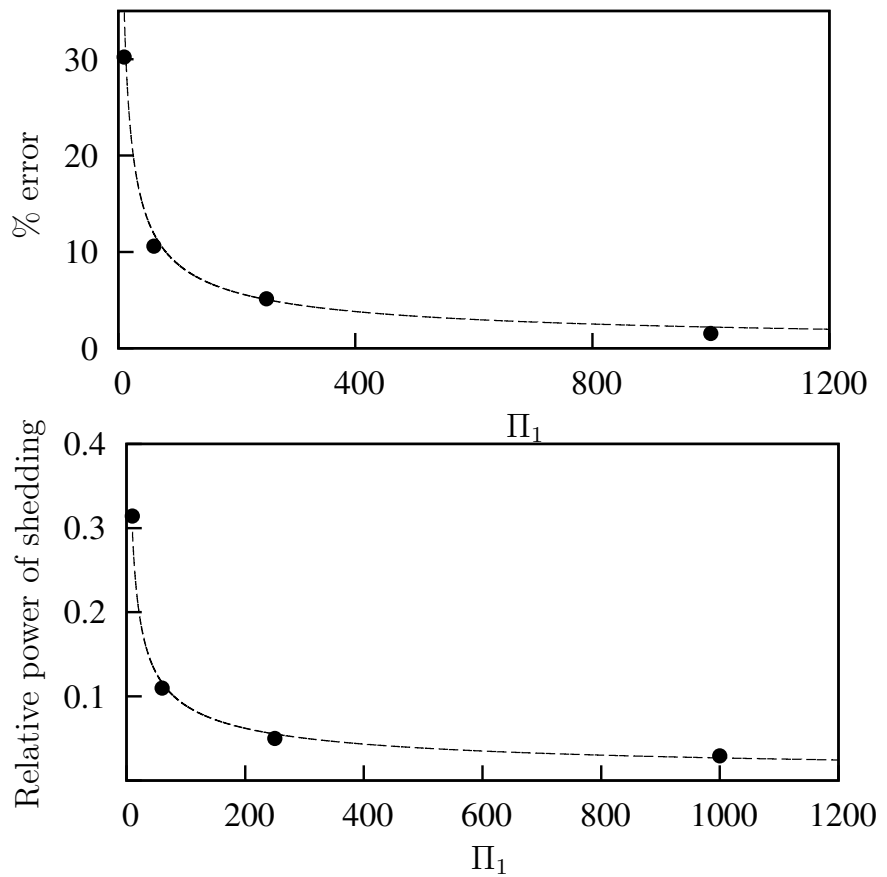
$$\% \text{ error} = \left| \frac{P_{m(QSS)} - P_{m(DNS)}}{P_{m(DNS)}} \right| \times 100.$$



Relative power of shedding and % error of power between QSS and DNS is an inverse function of Π_1

$$\% \text{ error} = \left| \frac{P_{m(QSS)} - P_{m(DNS)}}{P_{m(DNS)}} \right| \times 100.$$

$$\% \text{error} = 138.697 \Pi_1^{-0.6}$$

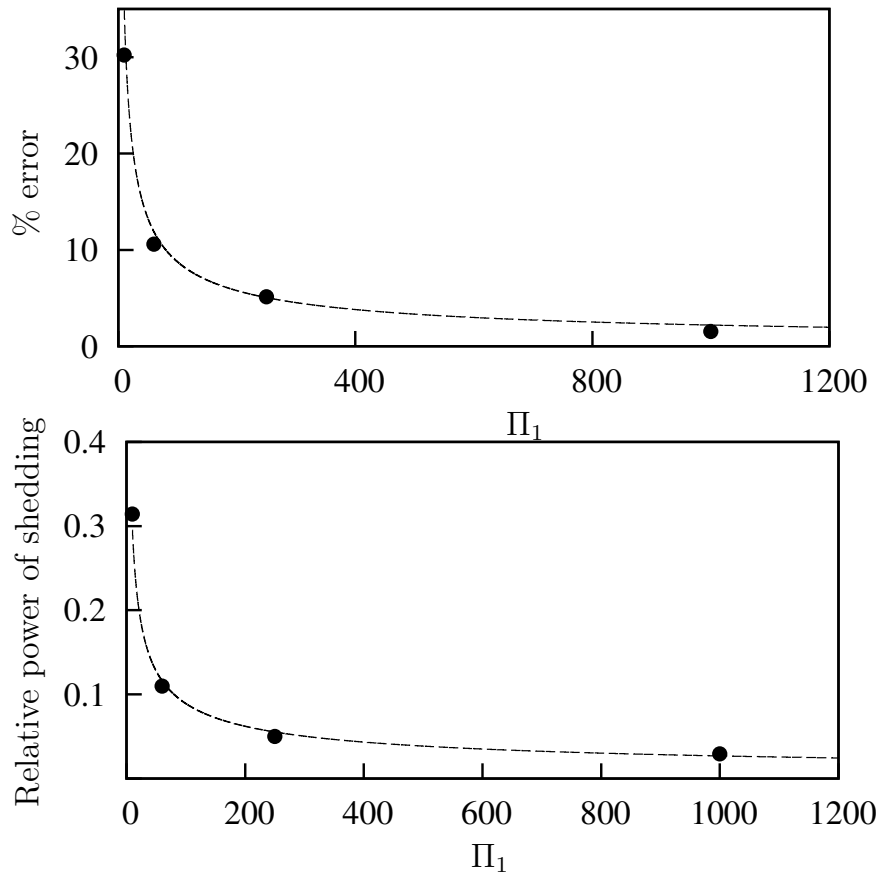


Relative power of shedding and % error of power between QSS and DNS is an inverse function of Π_1

$$\% \text{ error} = \left| \frac{P_{m(QSS)} - P_{m(DNS)}}{P_{m(DNS)}} \right| \times 100.$$

$$\% \text{error} = 138.697 \Pi_1^{-0.6}$$

$$\text{Relative power} = 0.977 \Pi_1^{-0.52}$$



Conclusions from phase 1

- Π_1 and Π_2 provide a good collapse compared to the classical VIV parameters, U^* and ζ .
- The velocity amplitude and the power transfer does not depend on the natural frequency of the system over a large range of frequencies.
- Quasi-steady state model provides a good prediction of power output in comparison with DNS data of the system when Π_1 is relatively high.
- As Π_1 is decreased, the deviation between QSS and DNS data increases as the influence of vortex shedding becomes more stronger.

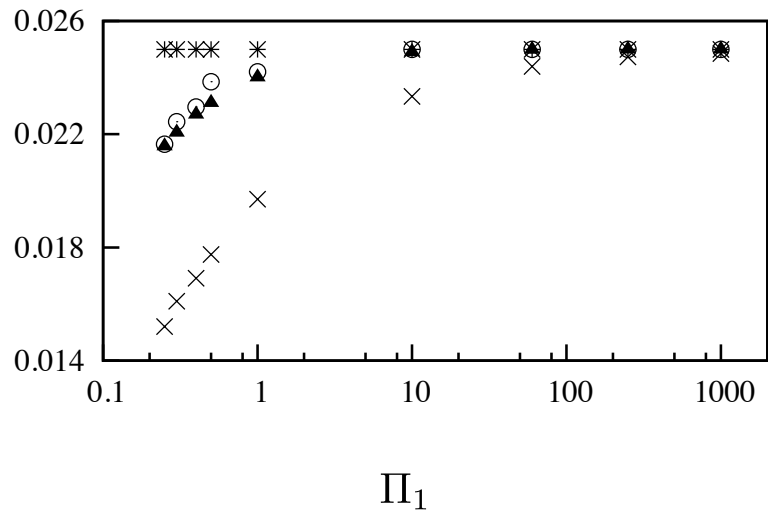
Effect of Π_1 and non-linear effects on galloping frequency

$$\frac{\lambda D}{U} = \frac{1}{2} \left(\Pi_2 - \frac{1}{2} \right) \pm \sqrt{\Pi_2^2 - \Pi_2 a_1 + \frac{a_1^2}{4} - 4\Pi_1}$$

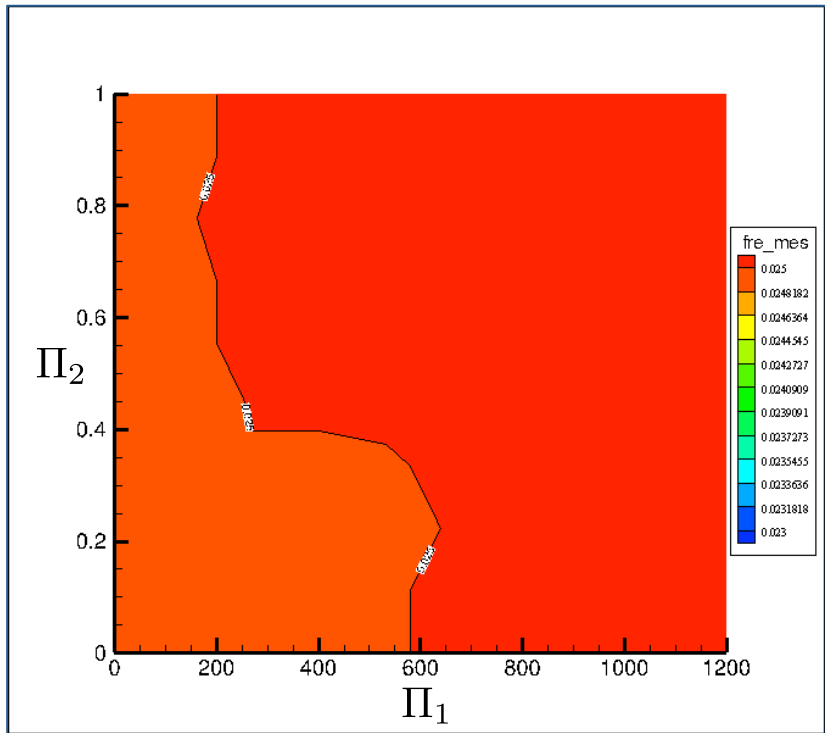
$$f_{input} = 0.025$$

- f_{input} (*)
- f_{linear} (○)
- f_{QSS} (▲)
- f_{DNS} (×)

$$\frac{fD}{U}$$

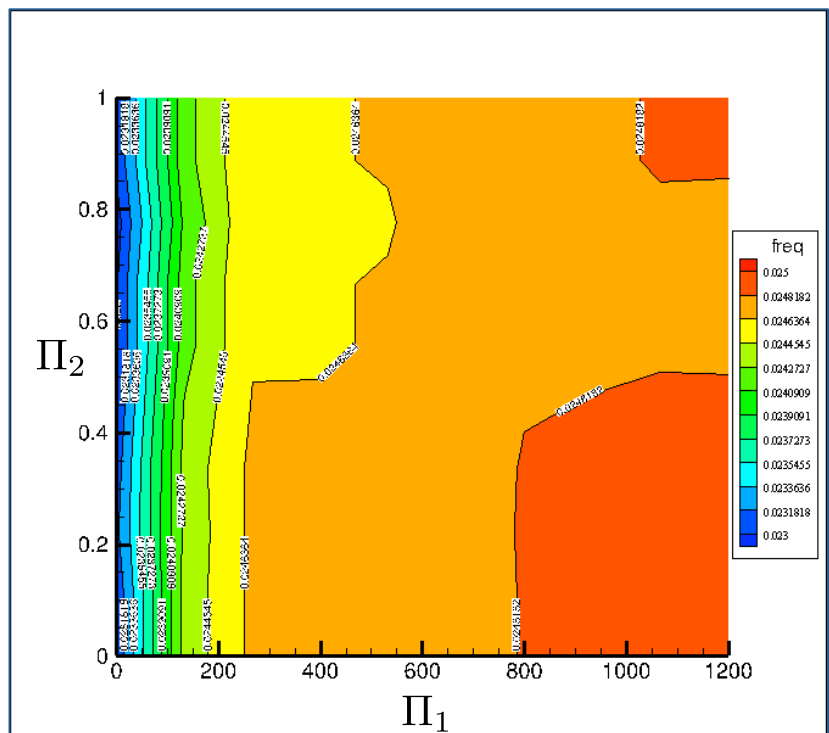


Frequency data in Π_1 and Π_2 space



QSS frequency data (freq_mes)

$$f_{input} = 0.025$$



DNS frequency data (freq)

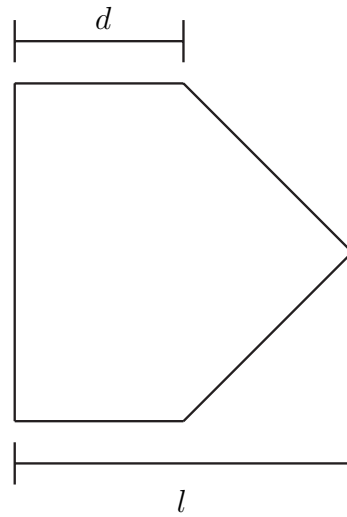


Conclusions from phase 2

- The linear frequency of the system could be obtained from the imaginary component of the eigenvalue equation of the linearised QSS model.
- This equation provides a good prediction of the frequency at high Π_1 . However, it deviates as Π_1 reduces due to non linear forcing.
- The linearised equation fails to predict the frequency at the point where the term under the square root positive. However, the general QSS model does output a frequency.
- The region where the linear expression of frequency fail could not be captured in the DNS data, as the vortex shedding becomes stronger and therefore suppresses galloping.

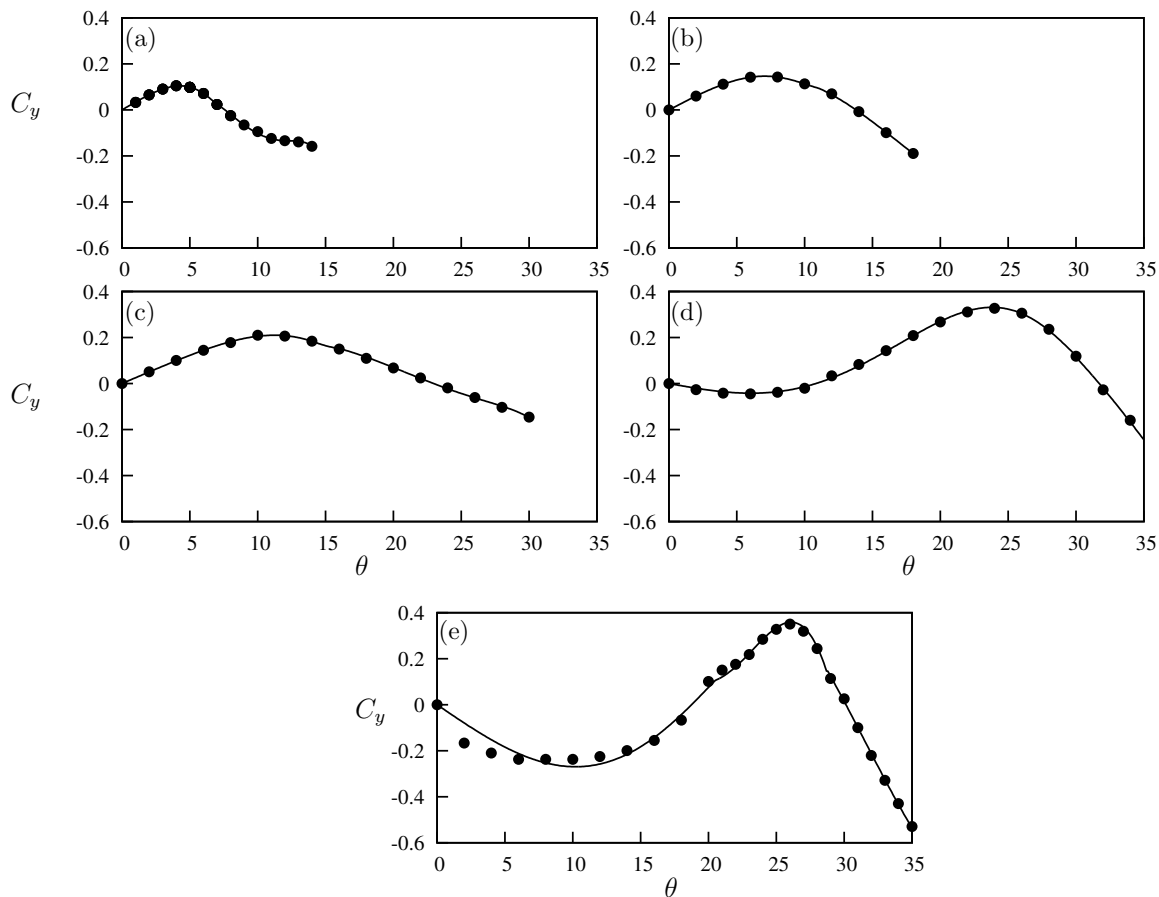


Delaying the shear layer re-attachment



Delaying the shear layer re-attachment

- (a) square
- (b) $\frac{d}{l} = 0.75$
- (c) $\frac{d}{l} = 0.5$
- (d) $\frac{d}{l} = 0.25$
- (e) triangle.

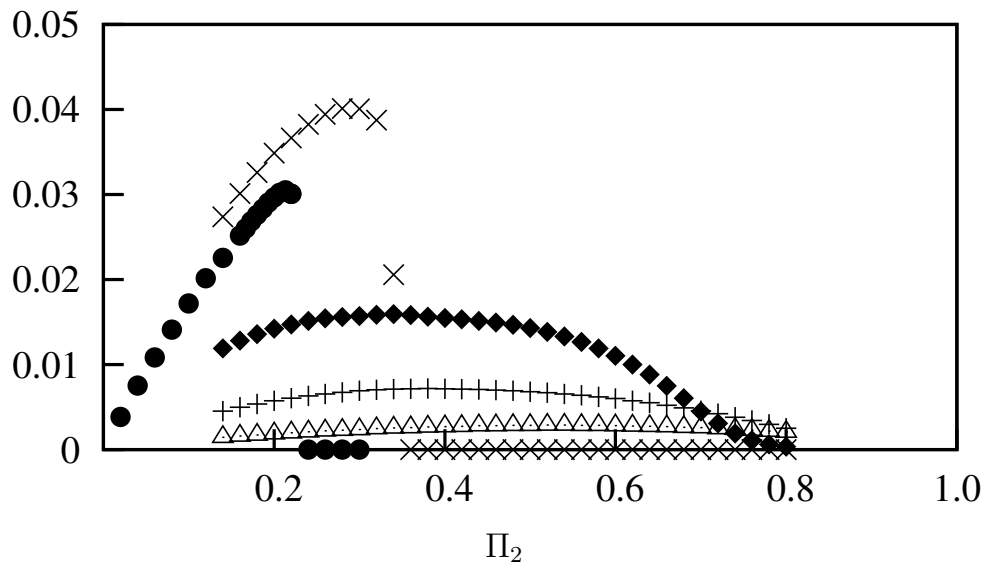


Dimensionless mean vs. Π_2 for five selected cross sections

$\frac{P_m}{\rho \mathcal{A} U^3}$

- square (\triangle)
- $\frac{d}{l} = 0.75$ $(+)$
- $\frac{d}{l} = 0.5$ (\blacklozenge)
- $\frac{d}{l} = 0.25$ (\times)
- triangle (\bullet)

QSS data at $Re = 200$, $\Pi_1 = 100$



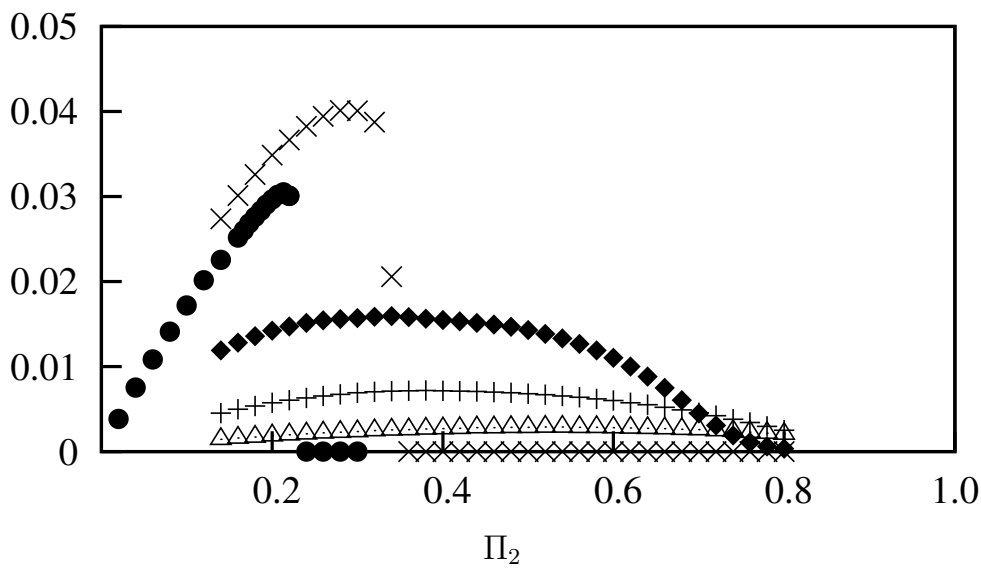
Dimensionless mean vs. Π_2 for five selected cross sections

The optimal ratio lies around

$$\frac{d}{l} = 0.25$$

- square (\triangle)
- $\frac{d}{l} = 0.75$ $(+)$
- $\frac{d}{l} = 0.5$ (\blacklozenge)
- $\frac{d}{l} = 0.25$ (\times)
- triangle (\bullet)

$$\frac{P_m}{\rho \mathcal{A} U^3}$$



QSS data at $Re = 200$, $\Pi_1 = 100$

Preliminary conclusions from phase 3

- Delaying the shear layer reattachment could lead to a higher power output. This was carried out by tapering away of the top and bottom surfaces of the square.
- As $\frac{d}{l}$ was reduced, a negative segment of the lift curve emerged which in return resulted in power transfer from the body to the fluid.
- Within the $\frac{d}{l}$ ratios tested, the optimal ratio lies around $\frac{d}{l} = 0.25$.



Publications

- Jayatunga, H.G.K.G., Tan B.T., Leontini J.S., A study on the energy transfer of a square prism under fluidelastic galloping. *Journal of Fluids and Structures* (2015),
<http://dx.doi.org/10.1016/j.jfluidstructs.2015.03.012>
- Leontini J.S., Zaho J., Jayatunga H.G.K.G., Lo Jacono D., Tan B.T., Sheridan J., 2014 'Frequency Selection and Phase Locking during Aeroelastic Galloping' presented to the 19th Australasian Fluid Mechanics Conference Melbourne, Australia 8-11 December 2014